

RESEARCH

Open Access



The plant-beneficial fungus *Trichoderma harzianum* T22 modulates plant metabolism and negatively affects *Nezara viridula*

Sara Van Hee^{1,2†}, Alejandro E. Segurado Luchsinger^{3,4†}, Antonino Cusumano⁵, Joleen Masschelein^{3,4}, Hans Jacquemyn^{2,6}, Bart Lievens^{1,2*} and Alejandro E. Segurado Luchsinger¹

Abstract

Background Plant-beneficial fungi play an important role in enhancing plant health and resistance against biotic and abiotic stresses. Although extensive research has focused on their role in eliciting plant defences against pathogens, their contribution to induced resistance against herbivorous insects and the underlying mechanisms remain poorly understood. In this study, we used insect bioassays and untargeted metabolomics to investigate the impact of root inoculation of sweet pepper with the plant-beneficial fungus *Trichoderma harzianum* T22 on direct defence responses against the insect herbivore *Nezara viridula*.

Results We observed reduced relative growth rate of *N. viridula* on leaves of fungus-inoculated plants, with no change in mortality. Untargeted metabolomic analyses revealed that inoculation with *T. harzianum* did not affect the leaf metabolome in the absence of herbivory five weeks after inoculation. However, compared to non-inoculated plants, inoculated plants exhibited significant metabolic alterations in herbivore-damaged leaves following *N. viridula* feeding, while changes in the metabolic profile of distant leaves were less pronounced. Notably, metabolites involved in the shikimate-phenylpropanoid pathway, known to be involved in plant defence responses, displayed higher accumulation in damaged leaves of inoculated plants compared to non-inoculated plants.

Conclusion Our results indicate that root inoculation with *T. harzianum* T22 affects plant defences against *N. viridula*, leading to reduced insect performance. Metabolite-level effects were primarily observed in damaged leaves, suggesting that the priming effect mainly results in localized metabolite accumulation at the site of attack. Future research should focus on identifying the detected compounds and determining their role in impairing *N. viridula* performance.

Keywords Defence priming, Herbivory, Metabolomics, Stink bug, Sweet pepper

[†]Sara Van Hee and Alejandro E. Segurado Luchsinger equally contributed to this work.

*Correspondence:

Bart Lievens

bart.lievens@kuleuven.be

¹CMPG Laboratory for Process Microbial Ecology and Bioinspirational Management (PME&BIM), Department of Microbial and Molecular Systems (M2S), KU Leuven, Willem de Croylaan 46 box 2458, B- 3001, Leuven, Belgium

²Leuven Plant Institute (LPI), KU Leuven, Leuven, Belgium

³Laboratory for Biomolecular Discovery and Engineering, Department of Biology, KU Leuven, Leuven, Belgium

⁴Center for Microbiology, VIB-KU Leuven, Leuven, Belgium

⁵Department of Agricultural, Food and Forest Sciences, University of Palermo, Palermo, Italy

⁶Laboratory of Plant Conservation and Population Biology, Department of Biology, KU Leuven, Leuven, Belgium



© The Author(s) 2025. **Open Access** This article is licensed under a Creative Commons Attribution-NonCommercial-NoDerivatives 4.0 International License, which permits any non-commercial use, sharing, distribution and reproduction in any medium or format, as long as you give appropriate credit to the original author(s) and the source, provide a link to the Creative Commons licence, and indicate if you modified the licensed material. You do not have permission under this licence to share adapted material derived from this article or parts of it. The images or other third party material in this article are included in the article's Creative Commons licence, unless indicated otherwise in a credit line to the material. If material is not included in the article's Creative Commons licence and your intended use is not permitted by statutory regulation or exceeds the permitted use, you will need to obtain permission directly from the copyright holder. To view a copy of this licence, visit <http://creativecommons.org/licenses/by-nc-nd/4.0/>.

Background

As sessile organisms, plants face constant threats from various attackers, including phytopathogens and herbivores. To withstand and counteract insect herbivores, plants have evolved a wide range of direct and indirect defence strategies [1, 2]. Direct defences involve plant traits that negatively affect herbivore performance, such as physical barriers (e.g. trichomes, thorns, spines, and thicker leaves) and defensive chemicals, while indirect defences rely on the attraction of the natural enemies of attacking herbivores [1, 2]. Both defence mechanisms can be constitutive or induced in response to herbivore damage [3]. Defence chemicals against herbivorous insects include a wide range of metabolites with repellent, anti-nutritive or toxic effects. These comprise specialised metabolites, such as glucosinolates, cyanogenic glucosides, terpenoids, alkaloids and phenolics, as well as non-proteinogenic amino acids [4]. In addition, plants produce a number of defence proteins that reduce the digestibility of plant tissue in the herbivore's gut, including proteinase inhibitors, α -amylase inhibitors and polyphenol oxidases [1]. These defence molecules are not only locally produced at the site of damage, but are often systemically circulated throughout the entire plant, allowing a plant-wide response to herbivory [3, 5].

Aside from interactions with insects, plants commonly engage in symbiotic relationships with microorganisms. In the rhizosphere, plants recruit a vast community of mutualistic microbes that provide essential benefits, such as improved nutrient acquisition and increased protection against (a)biotic stresses, including pest insects [6, 7]. For instance, many plant-beneficial fungi, such as mycorrhizal or endophytic fungi, promote plant growth by modulating hormonal pathways and enhancing nutrient uptake [6, 8–10]. In addition, several of these fungi can activate the plant's immune system, rendering the plant more resistant against a broad spectrum of attackers [11–13]. Generally, such induced resistance (IR) enables a faster and more efficient activation of plant defence responses upon a pathogen or herbivore attack [12, 14, 15]. These multifaceted properties of plant-beneficial fungi offer promising avenues for sustainable agriculture and have therefore sparked significant interest in the agricultural industry [8, 10, 16]. However, despite extensive research on the effects of plant-beneficial fungi on plant pathogens and associated mechanisms [10, 15, 17, 18], their impact on herbivorous insects, and particularly the underlying molecular mechanisms, remain less studied [19, 20].

Most mechanistic studies investigating the effects of plant-beneficial fungi on insect herbivores have focused on the molecular pathways activating the plant's defence responses using genome-wide and targeted gene expression profiling [21–25]. More recently, an increasing

number of studies have used targeted analysis of specialised metabolites with known activity against herbivores to elucidate their mode of action [25–28]. For instance, studies measuring phytohormone levels or quantifying specific toxic metabolites have been able to explain the enhanced defensive capability of plants inoculated with plant-beneficial fungi [20, 29, 30]. However, a broader and more comprehensive understanding of the metabolic reprogramming in host plants following inoculation with plant-beneficial fungi is still lacking (but see [31, 32]).

In this study, we assessed the impact of root inoculation with the plant-beneficial fungus *Trichoderma harzianum* T22 (recently reclassified as *Trichoderma afroharzianum* [33], but for consistency with previous studies further referred to as *T. harzianum*) on the performance of *Nezara viridula* (Hemiptera: Pentatomidae), also known as the southern green stink bug. An untargeted metabolomics approach was used to track changes in the plant's metabolic profile in response to fungal inoculation and insect feeding. This approach allows a comprehensive assessment of qualitative and (semi-)quantitative changes in the plant's secondary metabolism, offering a global fingerprint of its metabolic state [34, 35]. Specifically, we compared both local (herbivore-damaged tissue) and distant (undamaged tissue) metabolic responses to *N. viridula* feeding in inoculated and non-inoculated plants, while non-infested plants were included as a reference.

Trichoderma spp. (Hypocreales: Hypocreaceae) are among the most widespread and abundant root-associated beneficial microbes and are commonly used as biocontrol agents [8]. Their biocontrol activity relies on both direct antagonism, including parasitism, antibiosis or competition, and indirect, plant-mediated mechanisms through the induction of plant defences (induced resistance, IR) [8, 15]. These defence responses can enhance the plant's resilience not only to pathogens but also to herbivorous insects. *Trichoderma harzianum* T22, in particular, has demonstrated protective effects in a variety of crop systems, such as tomato and sweet pepper, showing efficacy against several arthropod herbivores, including aphids [31, 36], caterpillars [36, 37], spider mites [38], leaf miners [29] and stink bugs [23, 39]. These examples illustrate the broad potential of *Trichoderma* spp. in biocontrol strategies and support the rationale for investigating its effects on pest performance and plant metabolic responses in this study. *Nezara viridula* is an important pest species causing substantial damage to major open field crops like soybean and cotton. In recent years, it has emerged as an important pest in North-western Europe, where it poses a serious threat to greenhouse crops such as tomato, cucumber, eggplant, and sweet pepper, the model plant used in this study [40]. Current control methods are insufficient to manage this

pest, highlighting the necessity for more effective management strategies.

Results

Effects on stink bug performance

To evaluate the effects of *T. harzianum* T22 inoculation on sweet pepper resistance against *N. viridula*, we assessed its impact on nymphal growth rate, which serves as a good proxy for assessing indirect fungal effects on stink bug performance [41]. The relative growth rate of nymphs differed significantly between inoculated and non-inoculated plants (*t*-test, $t = 2.699$, $df = 26$, $p = 0.013$). On average, the relative growth rate of *N. viridula* nymphs on fungal-inoculated plants was 23.2%, while this was 37% on non-inoculated plants (Fig. 1a). On the contrary, mortality of the *N. viridula* nymphs was not affected by fungal inoculation (Fig. 1b; GLM, $\chi^2 = 0.328$, $df = 1$, $p = 0.567$).

Effects on the leaf metabolome

To investigate the potential mechanisms underlying the observed negative effects of *T. harzianum* T22 on *N. viridula*, an untargeted metabolomics analysis was performed. This analysis revealed a total of 3376 tentative compounds across the different samples analysed. Principal Compound Analysis (PCA) ordination, explaining 43.7% of the total variation (PC1: 28.9%; PC2: 14.8%), mainly separated local from distant leaves along the PC2 axis (Fig. 2a). PerMANOVA indicated that location ($p = 0.002$) and herbivory ($p = 0.002$), as well as their interaction ($p = 0.001$), significantly affected the metabolic profiles, while fungal inoculation did not (Table 1). When

limiting the PCA to local samples (PC1: 38.4%; PC2: 16.9%), more distinct grouping patterns were observed, with undamaged and damaged samples separating along PC1 (Fig. 2b). Furthermore, among the damaged local leaves, a clear separation was observed between *T. harzianum*-inoculated and non-inoculated plants. Samples from *T. harzianum*-inoculated plants grouped along PC1 between those from non-inoculated damaged plants and the group of all undamaged plants. In contrast, samples from undamaged *T. harzianum*-inoculated and non-inoculated plants showed substantial overlap in the PCA plot (Fig. 2b).

In the comparison of the metabolic profiles of local leaf samples from *T. harzianum*-inoculated and non-inoculated plants damaged by *N. viridula* feeding (TD-Loc versus CD-Loc; Fig. 3a, b), we found 68 differentially accumulated metabolites (DAMs). Of these, 29 were more abundant in the leaves of *Trichoderma*-inoculated plants, while 39 accumulated to higher levels in the leaves of control plants (Table 2). Although none of the metabolites could be identified at the compound level, 17 of these DAMs were classified using NPClassifier at the pathway, superclass and class level. The annotated metabolites that accumulated to higher levels in inoculated plants included one metabolite from the alkaloid pathway (superclass: ornithine alkaloids, class: polyamines), one from the amino acids and peptides pathway (superclass: oligopeptides, class: tripeptides) and one from the fatty acid pathway (superclass: glycerolipids, class: unclassified). Additionally, three metabolites were associated with the terpenoid pathway (superclass: diterpenoids, classes: kaurane and phyllocladane

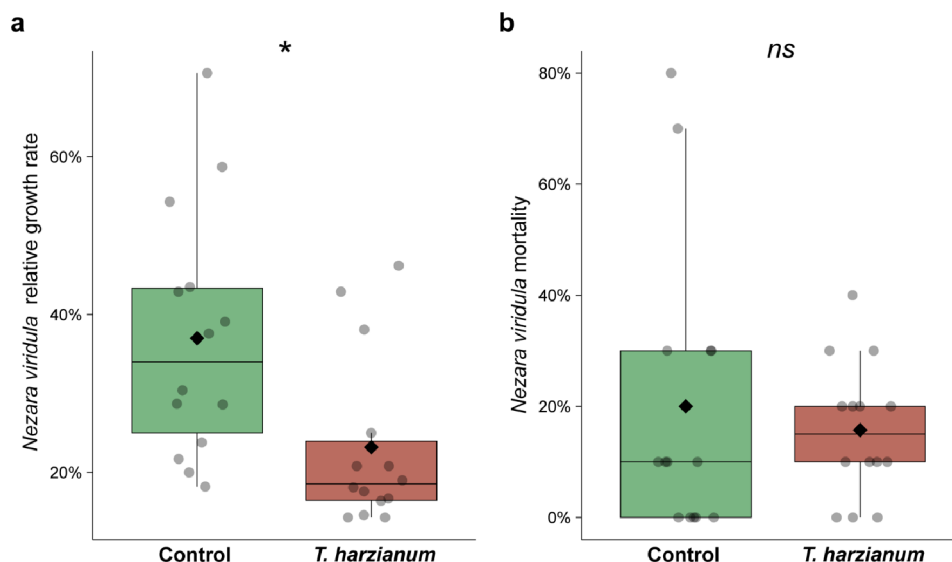


Fig. 1 Effects of inoculation of sweet pepper with *Trichoderma harzianum* T22 on (a) relative growth rate and (b) mortality of *Nezara viridula* 3rd instar nymphs, after feeding for one week on the plants. The lower, middle and upper lines of the boxplot correspond to the first quartile, median and third quartile, respectively, while the diamond represents the average. Data points represent the different replicates ($n = 14$). The asterisk represents a significant difference between the treatments ((a) *t*-test, $p < 0.05$; (b) GLM), while “ns” indicates no significant difference

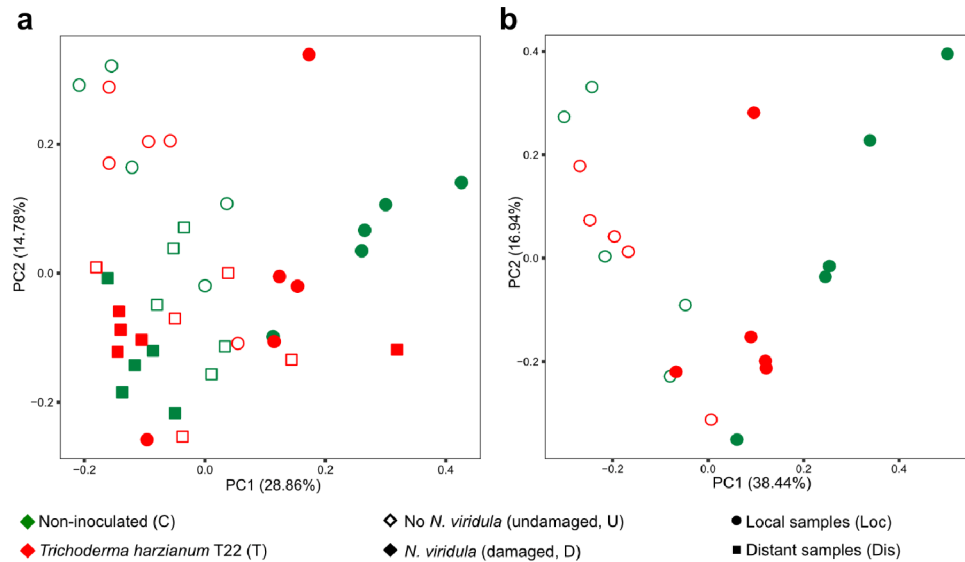


Fig. 2 General overview of the impact of *Trichoderma harzianum* T22 inoculation, *Nezara viridula* feeding and tissue location on the metabolome of sweet pepper leaves ($n=5$). For both *T. harzianum*-inoculated plants (T, red) and non-inoculated control plants (C, green), one leaf was enclosed in a mesh bag (local leaf), and infested with ten 3rd instar *N. viridula* nymphs (D (damaged), filled symbols) or non-infested (U (undamaged), empty symbols). One week later, local leaves (Loc, dots) and distant leaves (Dis, squares) were harvested, and the metabolic profile was analysed. **(a)** Principal component analysis (PCA) ordination plot of the metabolomes of all leaf samples. **(b)** PCA ordination plot of only the local leaf samples

Table 1 Results of PerMANOVA, based on Euclidean distances, for the factors “fungal inoculation”, “herbivory”, “location” and all interaction terms

Treatment	df	R ²	F	p-value ^a
Inoculation	1	0.032	1.623	0.089
Herbivory	1	0.087	4.453	0.002 **
Location	1	0.093	4.780	0.002 **
Inoculation × Herbivory	1	0.020	1.004	0.411
Inoculation × Location	1	0.024	1.212	0.248
Herbivory × Location	1	0.095	4.875	0.001 ***
Inoculation × Herbivory × Location	1	0.024	1.245	0.217

^a Significances are indicated with asterisks; **, 0.01 < p-value < 0.001; ***, 0 < p-value < 0.001

diterpenoids; colensane and clerodane diterpenoids; & superclass: monoterpenoids, class: iridoids monoterpenoids) and three with the shikimate-phenylpropanoid pathway (superclass: phenylpropanoids, class: cinnamic acids and derivatives; superclass: coumarins, class: simple coumarines; superclass: unclassified, class: chalcones) (Table 2). The metabolites that were present in higher amounts in the control plants included two metabolites from the alkaloid pathway (superclass: nicotinic acid alkaloids, class: pyridine alkaloids; superclass: histidine alkaloids, class: imidazole alkaloids), two from the amino acids and peptides pathway (superclass: small peptides, class: tripeptides; superclass: unclassified, class: amino-sugars), two from the carbohydrate pathway (superclass: nucleosides, classes: pyrimidine nucleoside; purine nucleoside), one from the fatty acid pathway (superclass: glycerophospholipids, class: glycerophosphocholines),

and one from the terpenoid pathway (superclass: monoterpenoids, class: menthane monoterpenoids) (Table 2). In the absence of *N. viridula* feeding, no differences in the metabolic profiles of local leaves were found between inoculated and non-inoculated plants (Fig. 3c), as is also evidenced by the overlap of the metabolomes in the PCA plot (Fig. 3d). When looking at the effects of fungal inoculation in response to *N. viridula* feeding in distant leaves, 14 metabolites displayed significantly higher accumulation in *T. harzianum*-inoculated plants compared to non-inoculated plants, while five compounds accumulated to higher amounts in non-inoculated plants (TD-Dis versus CD-Dis; Fig. 4a, b; Table S1 in Additional File 1). By contrast, no differences were detected between distant leaves of undamaged *T. harzianum*-inoculated and non-inoculated plants (TU-Dis versus CU-Dis; Fig. 4c, d).

Discussion
Our results revealed a significant reduction in the relative growth rate of *N. viridula* nymphs feeding on sweet pepper plants inoculated with *T. harzianum* T22 (from 23.2% on non-inoculated plants to 37% on inoculated plants), but no effects on nymph mortality. Although not assessed in this study, a delay in nymphal growth might implicate reduced feeding damage on the plant or could translate into negative effects on adult fitness and reproductive success [42, 43]. This hypothesis is supported by our previous research, in which we observed a reduction in *N. viridula* feeding damage on sweet pepper plants inoculated with *T. harzianum* T22 [39]. The observed

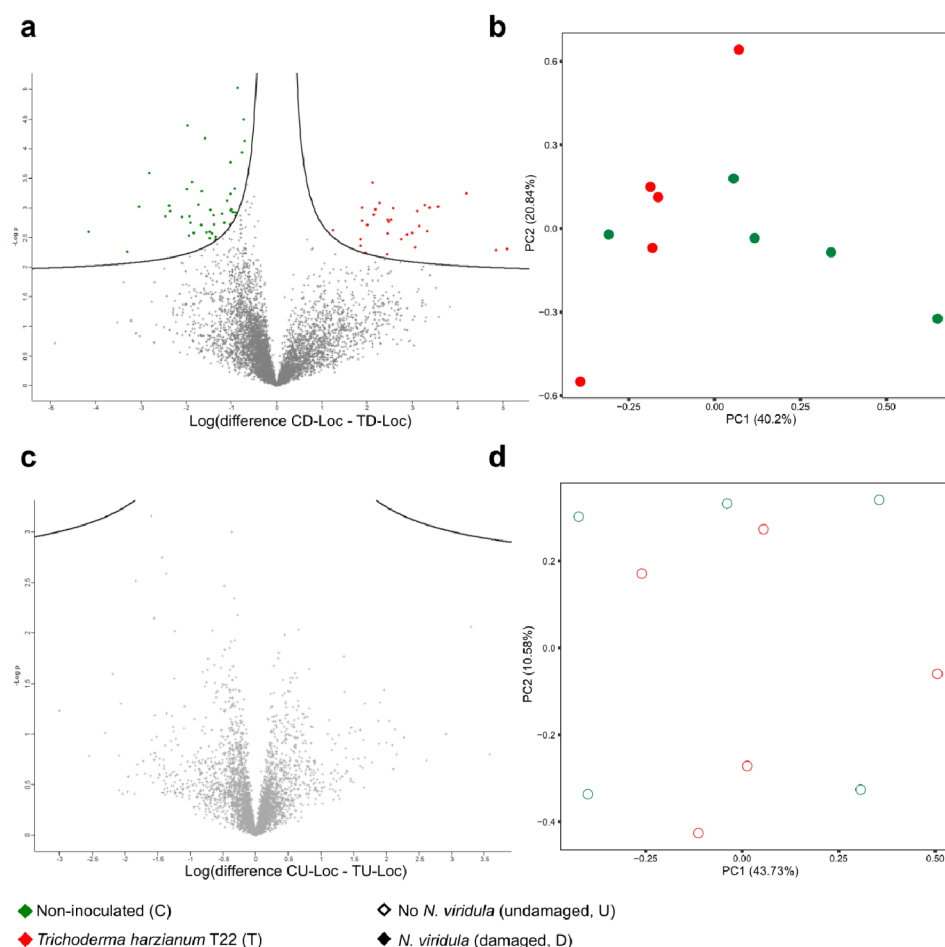


Fig. 3 Impact of *Trichoderma harzianum* T22 inoculation on the metabolome of local leaves from *Nezara viridula*-infested (a, b) or uninfested sweet pepper plants (c, d) ($n = 5$). (a) Volcano plot of damaged leaf samples from non-inoculated (CD-Loc, left side) and *T. harzianum*-inoculated plants (TD-Loc, right side). (b) Principal component analysis (PCA) plot of the metabolomes of local leaf samples from non-inoculated (green) and *T. harzianum*-inoculated damaged plants (red). (c) Volcano plot of undamaged leaf samples from non-inoculated (CU-Loc, left side) and *T. harzianum*-inoculated plants (TU-Loc, right side). (d) PCA plot of the metabolomes of local leaf samples from non-inoculated (green) and *T. harzianum*-inoculated (red) undamaged plants. The volcano plots display the t -test differences (log transformed) between the two treatments on the x-axis, and the negative logarithm of the t -test p -value on the y-axis. Coloured points on the left side of the line represent differentially accumulated metabolites (DAMs) with significantly higher accumulation in the left side treatment, while the coloured points on the right side of the line represent DAMs with significantly higher accumulation in the right-side treatment. Grey crosses indicate metabolites that do not show differential accumulation in any of the two treatments. The metabolomics features that showed the highest increase in one treatment compared with the other one are found towards the sides of the plot (on the left side in case of higher accumulation in (a) CD-Loc or (c) CU-Loc, on the right side in case of higher accumulation in (a) TD-Loc or (c) TU-Loc), while the most statistically significant metabolomics features are found towards the top of the volcano plot

reduction in relative growth rate is further supported by previous findings on tomato plants, where similar effects were reported for *N. viridula* nymphs [23]. Likewise, similar effects of *T. harzianum* T22 inoculation on indirect plant defences were shown in sweet pepper and tomato infested with *N. viridula* eggs, leading to enhanced attraction of the egg parasitoid *Trissolcus basalis* [44, 45]. Together, these studies demonstrate that the negative effects of *T. harzianum* T22 on *N. viridula* extend beyond a single host plant species. Furthermore, similar impacts on life-history traits have been reported for other arthropods, including aphids, spider mites, leaf miners and

caterpillars, following *T. harzianum* T22 inoculation [29, 31, 36–38], showing its great potential in pest control.

Negative effects on herbivores by plant-beneficial fungi are often attributed to the synthesis of plant defence-related compounds that are deterrent, anti-nutritive or toxic to herbivores [12, 46]. For instance, inoculation of maize with *Trichoderma atroviride* has been associated with the production of volatile oxylipins and jasmonic acid (JA)-related metabolites with activity against *Spodoptera frugiperda* larvae [20], while *T. harzianum* T22 increased JA- and salicylic acid (SA)-related metabolites involved in plant defence in tomato even in the

Table 2 Significant metabolomic features with putative annotation for local leaf samples of non-inoculated (CD-Loc) versus *Trichoderma Harzianum* T22-inoculated (TD-Loc), *Nezara viridula*-damaged plants. Metabolites are grouped according to in which treatment they accumulated to a higher level, and within each group according to their *q*-value

Feature ID ^a	m/z ^b	RT ^c	Molecular formula	Annotation pathway level ^d	Annotation superclass level ^d	Annotation class level ^d	Difference ^e	q-value ^f
Higher accumulation in CD-Loc versus TD-Loc								
1	200.2375	7.58	unknown ^g	unknown	unknown	unknown	-3.04	0.009
2	246.1449	3.21	unknown	unknown	unknown	unknown	-1.99	0.010
3	446.1592	1.24	unknown	unknown	unknown	unknown	-1.66	0.013
4	248.1242	2.18	unknown	unknown	unknown	unknown	-1.87	0.014
5	172.0606	3.36	unknown	unknown	unknown	unknown	-2.35	0.014
6	233.0423	1.83	unknown	unknown	unknown	unknown	-2.81	0.015
7	474.2924	5.33	C ₂₁ H ₃₉ N ₅ O ₇	Amino acids and peptides	Small peptides	Tripeptides	-2.38	0.015
8	207.1381	7.08	C ₁₃ H ₁₈ O ₂	Terpenoids	Monoterpenoids	Menthane terpenoids	-0.86	0.016
9	307.0938	4.45	unknown	unknown	unknown	unknown	-1.02	0.018
10	190.0712	3.36	unknown	unknown	unknown	unknown	-2.46	0.018
11	212.1396	1.98	unknown	unknown	unknown	unknown	-2.09	0.019
12	202.0870	6.64	unknown	unknown	unknown	unknown	-0.73	0.019
13	178.1341	5.97	C ₁₀ H ₁₅ N ₃	Alkaloids	Nicotinic acid alkaloids	Pyridine alkaloids	-4.16	0.019
14	130.0500	3.35	unknown	unknown	unknown	unknown	-1.73	0.019
15	89.0419	3.53	unknown	unknown	unknown	unknown	-1.58	0.020
16	237.1234	6.12	unknown	unknown	unknown	unknown	-1.93	0.023
17	247.0578	1.22	unknown	unknown	unknown	unknown	-1.91	0.027
18	258.1178	1.23	unknown	unknown	unknown	unknown	-1.47	0.027
19	312.0950	5.34	C ₁₁ H ₁₅ N ₅ O ₆	Carbohydrates	Nucleosides	Pyrimidine nucleosides	-0.77	0.028
20	258.1101	1.23	C ₈ H ₂₀ NO ₆ P	Fatty acids	Glycerophospholipids	Glycerophosphocholines	-1.66	0.028
21	129.1274	7.46	unknown	unknown	unknown	unknown	-0.93	0.029
22	164.0741	5.36	unknown	unknown	unknown	unknown	-1.01	0.029
23	225.1486	7.08	unknown	unknown	unknown	unknown	-0.71	0.029
24	260.1970	2.58	unknown	unknown	unknown	unknown	-1.10	0.029
25	69.0336	1.85	unknown	unknown	unknown	unknown	-1.40	0.030
26	263.0165	1.85	unknown	unknown	unknown	unknown	-1.94	0.030
27	260.1970	4.58	unknown	unknown	unknown	unknown	-1.21	0.031
28	162.0763	1.89	unknown	unknown	unknown	unknown	-1.84	0.031
29	232.1293	2.04	unknown	unknown	unknown	unknown	-1.39	0.034
30	258.1024	1.23	unknown	unknown	unknown	unknown	-3.30	0.036
31	460.2039	2.19	unknown	unknown	unknown	unknown	-1.55	0.038
32	188.9119	1.16	unknown	unknown	unknown	unknown	-1.48	0.038
33	244.0929	3.15	C ₉ H ₁₃ N ₃ O ₅	Carbohydrates	Nucleosides	Pyrimidine nucleosides	-1.02	0.038
34	112.0506	3.14	C ₄ H ₅ N ₃ O	Alkaloids	Histidine alkaloids	Imidazole alkaloids	-1.00	0.039
35	106.0499	1.17	unknown	unknown	unknown	unknown	-1.44	0.041
36	245.1861	6.62	unknown	unknown	unknown	unknown	-1.16	0.042
37	226.1310	1.85	unknown	unknown	unknown	unknown	-0.97	0.045
38	262.1400	4.91	unknown	unknown	unknown	unknown	-1.98	0.045
39	180.0868	1.82	C ₆ H ₁₃ NO ₅	Amino acids and peptides	(Small peptides)	Aminosugars	-1.48	0.045
Higher accumulation in TD-Loc versus CD-Loc								
40	317.2110	7.14	C ₂₀ H ₂₈ O ₃	Terpenoids	Diterpenoids	Colensane and clerodane diterpenoids	3.39	0.009
41	721.3299	7.13	unknown	unknown	unknown	unknown	3.28	0.011
42	299.2005	7.12	C ₂₀ H ₂₆ O ₂	Terpenoids	Diterpenoids	Kaurane and phyllocladane diterpenoids	3.57	0.012
43	761.3249	7.08	unknown	unknown	unknown	unknown	4.20	0.012
44	182.0539	6.00	unknown	unknown	unknown	unknown	2.19	0.013

Table 2 (continued)

Feature ID ^a	m/z ^b	RT ^c	Molecular formula	Annotation pathway level ^d	Annotation superclass level ^d	Annotation class level ^d	Difference ^e	q-value ^f
Higher accumulation in CD-Loc versus TD-Loc								
45	473.0393	5.99	unknown	unknown	unknown	unknown	2.28	0.014
46	513.2705	7.13	unknown	unknown	unknown	unknown	3.10	0.014
47	455.0809	5.99	C ₁₉ H ₂₀ O ₁₃	(Shikimates and phenylpropanoids) Terpenoids	Monoterpenoids	Iridoids monoterpenoids	2.57	0.014
48	85.2736	5.99	unknown	unknown	unknown	unknown	2.13	0.019
49	404.0834	5.98	unknown	unknown	unknown	unknown	2.45	0.019
50	360.1289	5.98	unknown	unknown	unknown	unknown	2.48	0.020
51	699.3196	7.13	C ₂₉ H ₅₆ O ₁₆	Fatty acids	Glycerolipids	(Acyclic monoterpenoids)	1.88	0.020
52	181.0497	5.99	C ₉ H ₈ O ₄	Shikimates and phenylpropanoids	Phenylpropanoids C6-C3	Cinnamic acids and derivatives	2.15	0.020
53	441.0131	6.00	unknown	unknown	unknown	unknown	3.16	0.020
54	341.0877	5.99	C ₁₅ H ₁₈ O ₉	Shikimates and phenylpropanoids	Coumarins	Simple coumarins	2.52	0.021
55	805.3310	7.40	C ₃₃ H ₅₄ N ₈ O ₁₁ S	Amino acids and peptides	Oligopeptides	Tripeptides	3.33	0.023
56	645.2921	7.57	unknown	unknown	unknown	unknown	3.00	0.026
57	449.1782	6.81	unknown	unknown	unknown	unknown	1.89	0.026
58	289.0895	4.43	unknown	unknown	unknown	unknown	2.01	0.026
59	229.1911	6.59	unknown	unknown	unknown	unknown	2.46	0.027
60	221.1900	7.15	unknown	unknown	unknown	unknown	2.89	0.028
61	220.1535	6.69	C ₈ H ₁₉ N ₄ O ₃	Alkaloids	Ornithine alkaloids	Polyamines	4.85	0.029
62	203.1796	7.12	unknown	unknown	unknown	unknown	2.76	0.030
63	148.0815	1.21	unknown	unknown	unknown	unknown	5.10	0.030
64	805.3289	7.56	unknown	unknown	unknown	unknown	3.06	0.031
65	205.1588	7.12	unknown	unknown	unknown	unknown	1.85	0.037
66	309.1191	6.48	unknown	unknown	unknown	unknown	1.85	0.045
67	285.1308	7.01	C ₁₈ H ₂₀ OS	Shikimates and phenylpropanoids	(Sesquiterpenoids)	Chalcones	1.25	0.045
68	187.1486	7.13	unknown	unknown	unknown	unknown	2.44	0.049

^a Feature ID is a number purely given for indexing purposes^b m/z = mass to charge ratio^c RT = retention time (in minutes)^d Preliminary putative annotation at the pathway, superclass and class level was performed using SIRIUS, based on Natural Products Classifier. Classifications shown in brackets indicate predictions flagged as highly unlikely, while the classification following the brackets reflects the manually overridden annotation^e Student's *t*-test difference^f Student's *t*-test *q*-value. *Q*-values are adjusted *P*-values using an optimised False Discovery Rate (FDR) approach^g No putative annotation could be assigned for metabolites labelled "unknown"

absence of herbivory [29]. In our study, in the absence of herbivory, no metabolome differences were observed between sweet pepper plants with and without *T. harzianum* T22 inoculation five weeks after inoculation. However, upon *N. viridula* infestation, 68 DAMs were identified in damaged local leaves, with 29 at higher levels and 39 at lower levels in inoculated plants. Distant effects were smaller, with 19 DAMs, of which 14 occurred in higher and five in lower amounts in inoculated plants. This pattern of increased production of certain metabolites alongside reductions in others supports the idea that the production of defence-related compounds generally occurs at the expense of other metabolites to balance

the costs of plant growth and defence [47–49]. Our findings align with Alinç et al. [44], who reported no differences in the volatilome of *T. harzianum* T22-inoculated and non-inoculated tomato plants, unless the plants were subjected to *N. viridula* feeding and egg deposition. Nevertheless, our results contrast with another study that showed metabolic differences between *T. harzianum*-inoculated and non-inoculated tomato plants in the absence of herbivory [31]. These discrepancies likely reflect differences in plant species and environmental conditions, as well as experimental methods such as inoculation method, sampling time and tissue type [31, 32].

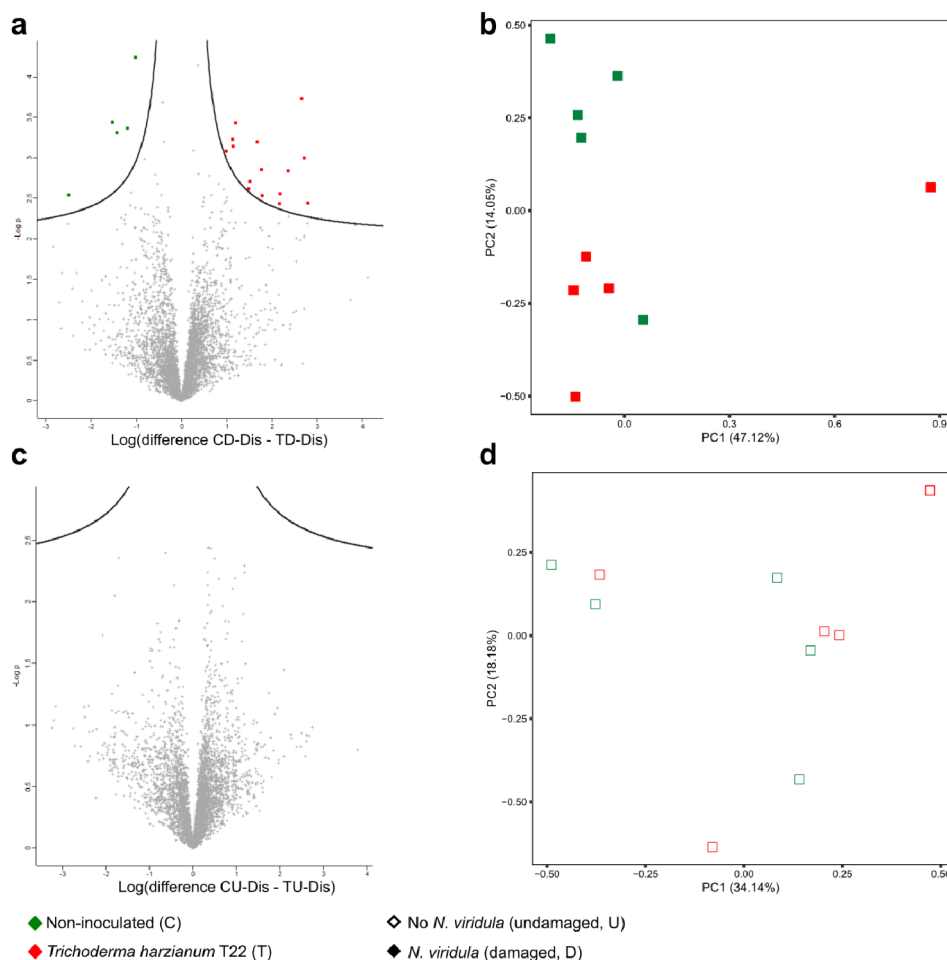


Fig. 4 Impact of *Trichoderma harzianum* T22 inoculation on the metabolome of distant leaves from *Nezara viridula*-infested (a, b) or uninfested sweet pepper plants (c, d) ($n=5$). (a) Volcano plot of damaged leaf samples from non-inoculated (CD_Dis, left side) and *T. harzianum*-inoculated plants (TD_Dis, right side). (b) Principal component analysis (PCA) plot of the metabolomes of distant leaf samples from non-inoculated (green) and *T. harzianum*-inoculated damaged plants (red). (c) Volcano plot of undamaged leaf samples from non-inoculated (CU_Dis, left side) and *T. harzianum*-inoculated plants (TU_Dis, right side). (d) PCA plot of the metabolomes of distant leaf samples from non-inoculated (green) and *T. harzianum*-inoculated (red) undamaged plants. The volcano plots display the t -test differences (log transformed) between the two treatments on the x-axis, and the negative logarithm of the t -test p -value on the y-axis. Coloured points on the left side of the line represent differentially accumulated metabolites (DAMs) with significant higher accumulation in the left side treatment, while the coloured points on the right side of the line represent DAMs with significant higher accumulation in the right-side treatment. Grey crosses indicate metabolites that do not show differential accumulation in any of the two treatments. The metabolomics features that showed the highest increase in one treatment compared with the other one are found towards the sides of the plot (on the left side in case of higher accumulation (a) CD_Dis or (c) CU_Dis, on the right side in case of higher accumulation in (a) TD_Dis or (c) TU_Dis), while the most statistically significant metabolomics features are found towards the top of the volcano plot

Our findings that the effects of *T. harzianum* T22 on the plant metabolome were only obvious in infested plants and that stink bug performance was reduced on fungus-inoculated plants suggest a priming effect of the fungus, leading to enhanced defence mechanisms when the plant is under attack [12, 50, 51]. Moreover, our multivariate analysis (PCA ordination) showed that the metabolomes of local leaves of inoculated damaged plants resembled those of undamaged plants more closely than those of non-inoculated damaged plants, suggesting that *T. harzianum* T22 buffers the overall metabolome reprogramming following *N. viridula* feeding. Although

no metabolite changes were observed in inoculated non-infested plants, it is important to note that a metabolome analysis provides only a snapshot of the plant's physiological state at the time of sampling, and primed responses can involve time-dependent (early and late) metabolic changes [49, 52–54]. Since we only sampled at one time-point, i.e. after five weeks of fungal inoculation and seven days of herbivore infestation, we lack insight into the temporal dynamics of the defence priming. Previous research has shown that in some cases, a primed state can persist throughout a plant's lifetime and can even be inherited by subsequent generations [51, 55].

Putative identification of the compounds involved in the fungus-induced modulation of the plant metabolism in local leaves after herbivory revealed three metabolites that are involved in the shikimate-phenylpropanoid pathway. This pathway, derived from the shikimate pathway, generates a diverse array of compounds, including phenylpropanoids, flavonoids, lignins, monolignols, phenolic acids, stilbenes and coumarins [56], which are involved in critical processes, such as cell division, hormonal regulation, photosynthesis, nutrient mineralization, and reproduction [57]. Moreover, several of these compounds are crucial for plant defence, acting as physical and chemical barriers against pathogen and herbivore attack, as well as serving as signal molecules for defence gene activation under biotic and abiotic stress [58]. Phenylpropanoids and their derivatives can be directly toxic to insect herbivores and serve as precursors to volatile organic compounds supporting indirect plant defence [59, 60]. In tomato, *T. harzianum* T22 has been shown to alter the plant metabolism by inducing the accumulation of phenylpropanoid pathway-related compounds, including phenylalanine, coumaric acid, chorismic acid, SA and SA-precursors or SA-related metabolites (both in the absence and presence of herbivory), precursors for phenylpropanoid synthesis [31], or through the accumulation of steroidal glycoalkaloids (in the absence of herbivory) such as α -tomatine which are considered to be important defensive metabolites against herbivores due to their toxic or deterring effects [32]. The metabolites induced by fungal inoculation following herbivory identified in our study belonging to the shikimate-phenylpropanoid or alkaloid pathway were predicted to represent simple coumarins, cinnamic acids and derivatives, chalcones, and polyamines. Certain coumarins exhibit toxic or anti-feedant effects, or oviposition deterrent effects on herbivorous insects [61, 62], while cinnamic acid derivatives possess antioxidant, antimicrobial and larvicidal activity [63]. Chalcones, a flavonoid subclass, are key in plant development and (a)biotic stress protection [1]. Polyamines contribute to growth, abiotic stress tolerance and likely plant immunity [64, 65]. Furthermore, we identified compounds involved in the terpenoids pathways, including the classes of iridoids monoterpenoids, kaurane and phyllocladane diterpenoids, and colandane and clerodane diterpenoids. These classes are known to contain many metabolites with antifeedant, insecticidal and antimicrobial properties [66, 67]. These compounds involved in the shikimate-phenylpropanoid, alkaloid or terpenoid pathway were not found in distant leaves, suggesting they are strongly determined by local herbivore presence.

Future research should focus on further identification of the DAMS identified in this study and their role in negatively affecting *N. viridula*. Therefore, integrating our data with a transcriptomics and targeted

metabolomics approach may provide us deeper insights into the complex interactions between plants, microbes and insects [31, 68]. Additionally, it is important to keep in mind the multicomponent nature of plant defence responses, phytochemicals often exhibit synergistic effects [69]. Furthermore, it may be valuable to examine not only the plant component, but also the insect side, more specifically the insect microbiome [70, 71]. Di Lelio et al. [37] recently demonstrated that *T. harzianum* T22 inoculation in tomato caused gut dysbiosis in *Spodoptera littoralis* caterpillars, disturbing the symbiosis with their gut microbiota and adversely affecting their development and survival [37]. The herbivore species studied in our study, *N. viridula*, also harbours a number of (obligate) symbionts, including *Sodalis* and *Pantoea*-like bacteria [72, 73]. Investigating how the alterations in the plant metabolome cascade up to the stink bug microbiome and metabolome, could provide novel insights into *Trichoderma*-mediated plant-insect interactions.

Conclusions

In conclusion, our study demonstrates that the plant-beneficial fungus *T. harzianum* T22 reduces the performance of *N. viridula* while altering sweet pepper metabolism in response to stink bug feeding. These effects were especially pronounced in local damaged leaves, where in particular compounds involved in the shikimate-phenylpropanoid pathway were more abundant in *Trichoderma*-inoculated plants. Results suggested that inoculation with *T. harzianum* T22 not only primes plants but also has a buffering effect on the overall metabolome reprogramming in damaged leaves in response to herbivory. Future work needs to be carried out to further identify the DAMs found in this study and investigate their role in impairing the performance of *N. viridula*.

Methods

Study organisms

This study was performed with *Trichoderma harzianum* T22, which is the main component in various biopesticides and biofertilizers, including Trianium-P (Koppert Biological Systems, The Netherlands). This strain was previously isolated by us from the commercial product Trianium-P and also used in our earlier research [39, 45, 74]. Since its isolation, the fungal strain has been stored at -80°C in 35% glycerol on potato dextrose agar (PDA) plugs until utilized in the experiments. Sweet pepper (*Capsicum annuum* L.; Solanaceae) cv 'IDS RZ F1' (seeds kindly provided by Rijk Zwaan, De Lier, The Netherlands) was used as the focal plant in this study. Plants were grown in a 3:1 mixture of potting mix (Universal potting mix; Agrofino, Gent, Belgium) and perlite under controlled conditions in a climate cabinet (MD1400, Snijders Labs, The Netherlands) at $23 \pm 1^{\circ}\text{C}$, $65 \pm 2\%$ RH, and

a 16L:8D photoperiod, with white LED lights providing a photosynthetic flux density of $790 \mu\text{mol photons m}^{-2} \text{s}^{-1}$. The *N. viridula* individuals used in the experiments were obtained from a lab culture maintained in insect cages ($47.5 \times 47.5 \times 47.5 \text{ cm}$) (BugDorm, MegaView Science Co. Ltd., Taiwan) under controlled conditions (ECL02, Snijders Labs, The Netherlands) at $25 \pm 1^\circ\text{C}$, $70 \pm 2\% \text{ RH}$, and a 16L:8D photoperiod. The lab culture originated from individuals acquired from the University of Palermo [23] and was yearly supplemented with newly field-caught individuals from Flanders (Belgium). Stink bugs were fed with seasonal organic vegetables (tomatoes, cabbage, and beans) and organic seeds (sunflower, soybean, and peanut) purchased from Colruyt Group (Halle, Belgium) and Bionoot (Zuidzwalde, The Netherlands), respectively. A wet cotton roll served as a water source, while sweet pepper plants (cv 'IDS RZ F1'), along with paper towels, were offered as oviposition substrates. Food and water were replenished every two to three days, and freshly laid eggs were systematically collected. Eggs and *N. viridula* nymphs emerging from the collected eggs were kept under the same conditions as described above and were used for maintaining the rearing process. The experiment was performed with third instar nymphs [38].

Fungal inoculum and plant inoculation

The preparation of fungal inoculum and subsequent plant inoculation followed procedures outlined in previous studies [39, 45, 75]. In summary, stored agar plugs containing mycelium of *T. harzianum* T22 were transferred onto PDA and incubated at 25°C for seven days. Next, sterile physiological saline solution (0.8% NaCl) was poured on the plates, and the spores were meticulously scraped off to form the fungal inoculum. To eliminate mycelial fragments, the spore suspensions underwent filtration through a microcloth (Mira Cloth, Merck, USA) and were washed three consecutive times with physiological saline solution. After determining the concentration of conidia with a Bürker hemocytometer, the spore suspensions were diluted to a final concentration of 1×10^7 conidia mL^{-1} . Prior to the experiments, conidial viability was assessed by plating a $100 \mu\text{L}$ aliquot of 1×10^3 conidia mL^{-1} on three PDA plates. After 24 h of incubation at 25°C , germinated and ungerminated conidia were counted under the microscope. Spores were considered germinated when the germ tube exceeded twice the spore diameter. The germination tests confirmed a viability rate of $> 90\%$ for all conidial suspensions used.

Plant inoculation took place at the first true leaf stage (BBCH stage 101). After rinsing the roots with tap water, they were immersed for 18 h in 10 mL of either the conidial spore suspension or physiological saline solution for non-inoculated control plants. Subsequently, seedlings were transplanted into 11 cm diameter plastic

pots (0.5 L) filled with the previously mentioned potting mixture. Plants were then placed under controlled conditions, as described earlier, ensuring no contact between inoculated and non-inoculated plants until further use in the experiments. This procedure leads to consistent plant inoculation and root colonization, as shown previously [39, 45, 75].

Nezara viridula performance bioassay

Stink bug performance was evaluated according to the procedures described by Ederli et al. [41]. Four weeks after fungal inoculation, the fourth true leaf of 14 plants per treatment was infested with ten third instar *N. viridula* nymphs that had been collectively weighed on an analytical balance prior to release. The leaf was subsequently enclosed in a fine white mesh bag ($13 \times 18 \text{ cm}$) and the bag was carefully closed around the petiole with a circular piece of sponge and cotton to prevent nymphal escape. Nymphs were allowed to feed on the leaf for one week (active feeding was visually confirmed), after which mortality and relative growth rate (RGR) of the nymphs were recorded. Relative growth rate (%) was calculated as $(\text{average final weight} - \text{average initial weight}) / \text{initial average weight} \times 100$, to account for possible differences in mortality [23, 41].

Leaf metabolome analysis

Immediately after evaluating insect performance (i.e. five weeks after fungal inoculation), from five plants per treatment the damaged leaf (the 4th true leaf; further referred to as "local leaf") and two undamaged leaves (the 5th and 6th true leaves sampled together and combined; further referred to as "distant leaves") were harvested and immediately flash-frozen in liquid nitrogen, before storing at -80°C until further use. A separate group of plants of the same age, incubated under identical conditions but without stink bug nymphs, had their fourth leaf enclosed in an empty mesh bag and were sampled similarly to serve as non-infested (undamaged) reference plants. An overview of all treatments sampled is given in Fig. 5.

Next, sampled leaves were ground in liquid nitrogen and subjected to an untargeted metabolomics approach performed by MS Omics (Denmark). To this end, crushed leaf material (50 mg) was diluted in extraction solvent (MeOH: H_2O , 80:20 ratio). The suspension was centrifuged at $10,000 \times g$ for 10 min at 4°C , and the supernatant was transferred into SpinX filters and filtrated by centrifugation at $15,000 \times g$ for 5 min at 4°C . Next, $5 \mu\text{L}$ of the filtered supernatant was injected into a UPLC system (Vanquish; Thermo Fisher Scientific, USA) coupled to a high-resolution quadrupole-orbitrap mass spectrometer (Q Exactive HF MS; Thermo Fisher Scientific, USA). The UPLC was performed using a slightly modified version of the protocol described in [76], as

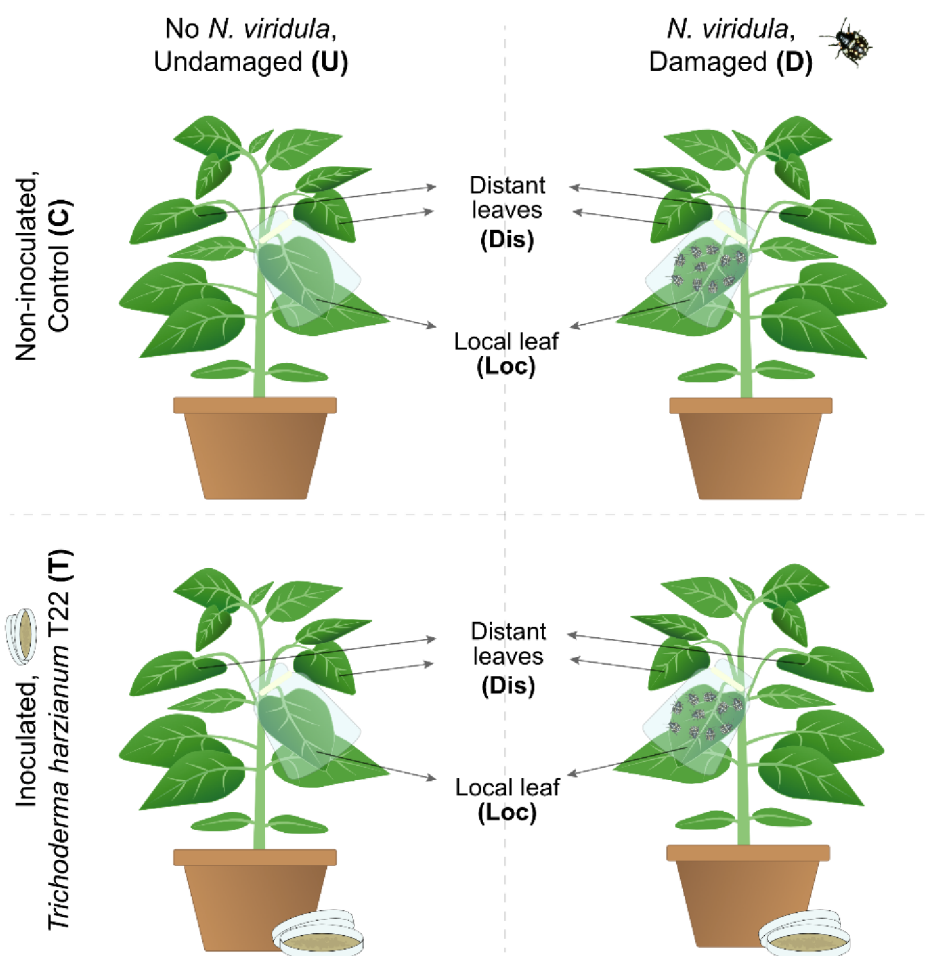


Fig. 5 Overview of the different treatments sampled and analysed in the untargeted metabolome analysis. Specifically, from infested (D) *Trichoderma harzianum* T22-inoculated (T) and non-inoculated control (C) plants, the leaf damaged by *Nezara viridula* (i.e., 4th true leaf; “local leaf” (Loc)) and two undamaged leaves (the 5th and 6th true leaves; “distant leaves” (Dis)) were harvested and analysed. An additional set of equally old plants that were not subjected to stink bug damage (U) but on which the fourth leaf was enclosed in an empty mesh bag, were included to serve as non-infested (undamaged) reference plants. The letters between brackets are also used in the presentation of the results

follows. LC separation was performed using an UPLC Acquity HSS T3 column (2.1 × 150 mm) with a 1.8 μm particle size (Waters, USA), held at 30 °C. The mobile phases consisted of (A) ammonium formate (10 mM) with 0.1% HCOOH in water, and (B) ammonium formate (10 mM) with 0.1% HCOOH in methanol. The analytes were eluted, while maintaining a constant flow rate of 300 μL min⁻¹, applying a multi-step gradient for solution B: 0–2 min, 0%; 2–4 min, 35%; 4–6 min, 90%; 6–14 min, 90%; 14–15 min, 0%. An electrospray ionization (ESI) interface was used as ionization source, and the analysis was performed in negative and positive ionization mode.

Raw data files were converted to.mzML format using MSConvert (ProteoWizard) [77], using the peak picking filter (with the vendor level msLevel set 1–2) to ensure centroided data. The.mzML files in positive and negative modes were uploaded and processed in MZmine3 (mzio) and we followed the recommendations for an LC-MS

set up presented by Heuckeroth et al. [78]. In short, we applied the following steps for the data pre-processing: Mass detection for MS1 and MS2 levels, Chromatogram building and resolving (EIC (extracted ion chromatogram) building, smoothing and EIC resolving [79]), ¹³C isotope filtering, sample alignment, gap-filling across the samples, filtering (duplicate filter and conditional row filter) and a feature grouping (metaCorrelated, Ion Identity networking and molecular networking). Filtering steps were applied to reduce the noise and uninformative features. A table with all the values used in this pre-processing pipeline can be found in Table S2 (Additional File 1). As a rule of thumb, we aimed to keep the feature count below 10,000 features. Processed tables were then exported for downstream analysis [80]. For statistical analysis in PERSEUS, the peak height was used in the quantification table. For molecular networking, and compound annotation, formula prediction and de-replication

in GNPS and SIRIUS, the area under the peak was used for the quantification table in GNPS. Conversely, .mgf files were used in both tools. The feature table can be found in Additional File 1 (Table S3). Finally, Cytoscape was used to visualize the molecular networks and to integrate the results from SIRIUS and PERSEUS onto the network by using the feature IDs as indexes.

Statistical analysis

To test whether inoculation with *T. harzianum* T22 affected the stink bug's relative growth rate, a two-sample *t*-test with unequal variances, also known as Welch's *t*-test, was used in R version 3.6.3 [81]. Differences in mortality were assessed using a generalized linear model (GLM) based on a negative binomial distribution. For statistical analysis of the metabolites data, the pre-processed feature table was exported into a .csv file using the feature intensities height. Afterwards, quantification tables from negative and positive mode were merged into a single feature quantification table. The software used for the statistical analysis was the PERSEUS computational platform (MaxQuant) [82, 83]. Data transformation methods were explored to standardize all variables, reduce redundancy, and correct for measurement errors [80, 84]. In short, data was transformed by renaming and grouping the variables according to the treatment, samples intensities were log2 transformed and filtered with an 80% threshold for valid values. Afterwards, imputation was performed to get rid of the NA values and normalization was achieved by subtracting the median to reduce the effects of the outliers within the dataset. An initial histogram check ensured that the data followed a normal distribution with an acceptable level of imputed values. PCA analysis (PCA visualizations were carried out in R) was used to highlight trends and groupings between samples and to check if there were any apparent batch effects (technical factors that affect variation in the data because of analysis of the samples in batches) in the dataset. Therefore, we used it as an extra quality control step. Two parametric tests were used to compare and record feature variations across treatments, False Discovery Rate (FDR < 0.05) was applied to correct for multiple testing. To compare pairs of treatments, *t*-test was used (e.g., Control versus *T. harzianum*) and to generate Volcano plots that would illustrate differentially accumulated metabolites when two treatments were compared. Volcano plots were created based on the (log-transformed) *t*-test difference (x-axis) and the (negative logarithm of the) *t*-test *p*-value (y-axis). In addition, permutational multivariate variance of analysis (perMANOVA) was performed to evaluate whether the variation in the data can be explained by the grouping variables and to test whether the centroids of the groups in the multivariate space differ significantly. The Euclidean distance was used, based on 1000 permutations, using the *adonis2* function of the R package *vegan* [85].

Supplementary Information

The online version contains supplementary material available at <https://doi.org/10.1186/s12870-025-06650-3>.

Supplementary Material 1

Acknowledgements

We are grateful to Rijk Zwaan (De Lier, The Netherlands) for providing sweet pepper seeds used in this research.

Author contributions

SVH, HJ and BL contributed to the study conception and experimental design, with input from AC. SVH performed the experiments and collected the data. AESL performed the processing and statistical analysis of the metabolomics data. Data visualization was done by SVH and AESL. JM and BL provided resources (materials, analysis tools and infrastructure). JM, HJ and BL contributed to project supervision and funding acquisition. SVH and AESL wrote the first draft of the manuscript, and all co-authors provided scientific and editorial input to the manuscript drafts. All authors have read and approved the manuscript for publication.

Funding

This work was funded by KU Leuven internal funds (grant C24E/19/052 to BL).

Data availability

The data supporting the findings of this study are included within the article (and its additional files).

Declarations

Ethics approval and consent to participate

Not applicable.

Consent for publication

Not applicable.

Competing interests

The authors declare no competing interests.

Received: 19 February 2025 / Accepted: 29 April 2025

Published online: 10 May 2025

References

1. War AR, Paulraj MG, Ahmad T, Buhroo AA, Hussain B, Ignacimuthu S, et al. Mechanisms of plant defense against insect herbivores. *Plant Signal Behav.* 2012;7:1306–20. <https://doi.org/10.4161/psb.21663>.
2. Dicke M, Baldwin IT. The evolutionary context for herbivore-induced plant volatiles: beyond the cry for help. *Trends Plant Sci.* 2010;15:167–75. <https://doi.org/10.1016/j.tplants.2009.12.002>.
3. Gatehouse JA. Plant resistance towards insect herbivores: A dynamic interaction. *New Phytol.* 2002;156:145–69. <https://doi.org/10.1046/j.1469-8137.2002.00519.x>.
4. Howe GA, Jander G. Plant immunity to insect herbivores. *Annu Rev Plant Biol.* 2008;59:41–66. <https://doi.org/10.1146/annurev.arplant.59.032607.092825>.
5. Wu J, Baldwin IT. New insights into plant responses to the attack from insect herbivores. *Annu Rev Genet.* 2010;44:1–24. <https://doi.org/10.1146/annurev-genet-102209-163500>.
6. Pineda A, Zheng SJ, van Loon JJA, Pieterse CMJ, Dicke M. Helping plants to deal with insects: the role of beneficial soil-borne microbes. *Trends Plant Sci.* 2010;15:507–14. <https://doi.org/10.1016/j.tplants.2010.05.007>.
7. Shikano I, Rosa C, Tan CW, Felton GW. Tritrophic interactions: microbe-mediated plant effects on insect herbivores. *Annu Rev Phytopathol.* 2017;55:313–31. <https://doi.org/10.1146/annurev-phyto-080516-035319>.
8. Woo SL, Hermosa R, Lorito M, Monte E. *Trichoderma*: a multipurpose, plant-beneficial microorganism for eco-sustainable agriculture. *Nat Rev Microbiol.* 2023;21:312–26. <https://doi.org/10.1038/s41579-022-00819-5>.

9. Harman GE, Howell CR, Viterbo A, Chet I, Lorito M. *Trichoderma* species — opportunistic, avirulent plant symbionts. *Nat Rev Microbiol*. 2004;2:43–56. <https://doi.org/10.1038/nrmicro797>.
10. Berg G. Plant–microbe interactions promoting plant growth and health: perspectives for controlled use of microorganisms in agriculture. *Appl Microbiol Biotechnol*. 2009;84:11–8. <https://doi.org/10.1007/s00253-009-2092-7>.
11. Van Wees SC, Van der Ent S, Pieterse CM. Plant immune responses triggered by beneficial microbes. *Curr Opin Plant Biol*. 2008;11:443–8. <https://doi.org/10.1016/j.pbi.2008.05.005>.
12. Pieterse CMJ, Zamioudis C, Berendsen RL, Weller DM, Van Wees SCM, Bakker PAHM. Induced systemic resistance by beneficial microbes. *Annu Rev Phytopathol*. 2014;52:347–75. <https://doi.org/10.1146/annurev-phyto-082712-102340>.
13. Jung SC, Martínez-Medina A, López-Raez JA, Pozo MJ. Mycorrhiza-induced resistance and priming of plant defenses. *J Chem Ecol*. 2012;38:651–64. <https://doi.org/10.1007/s10886-012-0134-6>.
14. De Kessel J, Conrath U, Flors V, Luna E, Mageroy MH, Mauch-Mani B, et al. The induced resistance lexicon: Do's and Don'ts. *Trends Plant Sci*. 2021;685–91. <https://doi.org/10.1016/j.tplants.2021.01.001>.
15. Martínez-Medina A, Pozo MJ, Cammue BPA, Vos CMF. Belowground defence strategies in plants: the plant–*Trichoderma* dialogue. Belowground defence strategies in plants. Springer Berlin Heidelberg. 2016. pp. 301–27. https://doi.org/10.1007/978-3-319-42319-7_13.
16. Berg G, Grube M, Schloter M, Smalla K. Unraveling the plant microbiome: looking back and future perspectives. *Front Microbiol*. 2014;5:1–7. <https://doi.org/10.3389/fmicb.2014.00148>.
17. Lorito M, Woo SL, Harman GE, Monte E. Translational research on *Trichoderma*: from 'omics to the field. *Annu Rev Phytopathol*. 2010;48:395–417. <https://doi.org/10.1146/annurev-phyto-073009-114314>.
18. Latz MAC, Jensen B, Collinge DB, Jørgensen HJL. Endophytic fungi as biocontrol agents: elucidating mechanisms in disease suppression. *Plant Ecol Divers*. 2018;11:555–67. <https://doi.org/10.1080/17550874.2018.1534146>.
19. Pappas ML, Samaras K, Koufakis I, Broufak G. Beneficial soil microbes negatively affect spider mites and aphids in pepper. *Agronomy*. 2021;11:1831. <https://doi.org/10.3390/agronomy11091831>.
20. Contreras-Cornejo HA, Macías-Rodríguez L, Del-Val E, Larsen J. The root endophytic fungus *Trichoderma atroviride* induces foliar herbivory resistance in maize plants. *Appl Soil Ecol*. 2018;124:45–53. <https://doi.org/10.1016/j.apsoil.2017.10.004>.
21. Posada-Vergara C, Lohaus K, Alhussein M, Vidal S, Rostás M. Root colonization by fungal entomopathogen systemically primes belowground plant defense against cabbage root fly. *J Fungi*. 2022;8:969. <https://doi.org/10.3390/jof8090969>.
22. Pappas ML, Liapoura M, Papantoniou D, Avramidou M, Kavroulakis N, Weinhold A, et al. The beneficial endophytic fungus *Fusarium Solani* strain K alters tomato responses against spider mites to the benefit of the plant. *Front Plant Sci*. 2018;9. <https://doi.org/10.3389/fpls.2018.01603>.
23. Alinç T, Cusumano A, Peri E, Torta L, Colazza S. *Trichoderma harzianum* strain T22 modulates direct defense of tomato plants in response to *Nezara viridula* feeding activity. *J Chem Ecol*. 2021;47:455–62. <https://doi.org/10.1007/s10886-021-01260-3>.
24. Lang B, Chen J. *Trichoderma harzianum* cellulase gene *thph2* affects *Trichoderma* root colonization and induces resistance to Southern leaf blight in maize. *J Fungi*. 2023;9:1168. <https://doi.org/10.3390/jof9121168>.
25. Raad M, Glare TR, Brochero HL, Müller C, Rostás M. Transcriptional reprogramming of *Arabidopsis thaliana* defence pathways by the entomopathogen *Beauveria bassiana* correlates with resistance against a fungal pathogen but not against insects. *Front Microbiol*. 2019;10:1–17. <https://doi.org/10.3389/fmicb.2019.00615>.
26. Rasool S, Vidkjær NH, Hooshmand K, Jensen B, Fomsgaard IS, Meyling NV. Seed inoculations with entomopathogenic fungi affect aphid populations coinciding with modulation of plant secondary metabolite profiles across plant families. *New Phytol*. 2021;229:1715–27. <https://doi.org/10.1111/nph.16979>.
27. Fontana A, Reichelt M, Hempel S, Gershenzon J, Unsicker SB. The effects of arbuscular mycorrhizal fungi on direct and indirect defense metabolites of *Plantago lanceolata* L. *J Chem Ecol*. 2009;35:833–43. <https://doi.org/10.1007/s10886-009-9654-0>.
28. Rasool S, Cárdenas PD, Pattison DI, Jensen B, Meyling NV. Isolate-specific effect of entomopathogenic endophytic fungi on population growth of two-spotted spider mite (*Tetranychus urticae* Koch) and levels of steroidal glycoalkaloids in tomato. *J Chem Ecol*. 2021;47:476–88. <https://doi.org/10.1007/s10886-021-01265-y>.
29. Aprile AM, Coppola M, Turrà D, Vitale S, Cascone P, Diletto G, et al. Combination of the systemin peptide with the beneficial fungus *Trichoderma afroharzianum* T22 improves plant defense responses against pests and diseases. *J Plant Interact*. 2022;17:569–79. <https://doi.org/10.1080/17429145.2022.2072528>.
30. Martínez-Medina A, Del Mar Alguacil M, Pascual JA, Van Wees SCM. Phytohormone profiles induced by *Trichoderma* isolates correspond with their biocontrol and plant growth-promoting activity on melon plants. *J Chem Ecol*. 2014;40:804–15. <https://doi.org/10.1007/s10886-014-0478-1>.
31. Coppola M, Diletto G, Digilio MC, Woo SL, Giuliano G, Molisso D, et al. Transcriptome and metabolome reprogramming in tomato plants by *Trichoderma harzianum* strain T22 primes and enhances defense responses against aphids. *Front Physiol*. 2019;10:745. <https://doi.org/10.3389/fphys.2019.00745>.
32. Papantoniou D, Vergara F, Weinhold A, Quijano T, Khakimov B, Pattison DI, et al. Cascading effects of root microbial symbiosis on the development and metabolome of the insect herbivore *Manduca sexta* L. *Metabolites*. 2021;11:731. <https://doi.org/10.3390/metabo11110731>.
33. Chaverri P, Branco-Rocha F, Jaklitsch W, Gazis R, Degenkolb T, Samuels GJ. Systematics of the *Trichoderma harzianum* species complex and the re-identification of commercial biocontrol strains. *Mycologia*. 2015;107:558–90. <https://doi.org/10.3852/14-147>.
34. De Vos RCH, Moco S, Lommen A, Keurentjes JJB, Bino RJ, Hall RD. Untargeted large-scale plant metabolomics using liquid chromatography coupled to mass spectrometry. *Nat Protoc*. 2007;2:778–91. <https://doi.org/10.1038/nprot.2007.95>.
35. Perez de Souza L, Alseekh S, Naake T, Fernie A. Mass spectrometry-based untargeted plant metabolomics. *Curr Protoc Plant Biol*. 2019;4:e20100. <https://doi.org/10.1002/cppb.20100>.
36. Di Lelio I, Coppola M, Comite E, Molisso D, Lorito M, Woo SL, et al. Temperature differentially influences the capacity of *Trichoderma* species to induce plant defense responses in tomato against insect pests. *Front Plant Sci*. 2021;12:678830. <https://doi.org/10.3389/fpls.2021.678830>.
37. Di Lelio I, Forni G, Magoga G, Brunetti M, Bruno D, Becchimanzi A, et al. A soil fungus confers plant resistance against a phytophagous insect by disrupting the symbiotic role of its gut microbiota. *Proc Natl Acad Sci*. 2023;120:2017. <https://doi.org/10.1073/pnas.2216922120>.
38. Samaras K, Mourtiadou S, Arampatzis T, Kakagianni M, Feka M, Wäckers F, et al. Plant-mediated effects of beneficial microbes and a plant strengthener against spider mites in tomato. *Plants*. 2023;12:938. <https://doi.org/10.3390/plants12040938>.
39. Van Hee S, Stockmans I, Alinç T, Cusumano A, Jacquemyn H, Lievens B. Effects of plant-beneficial fungi on plant growth and herbivore resistance under contrasting fertilizer conditions. *Plant Soil*. 2023;493:157–72. <https://doi.org/10.1007/s11104-023-06220-2>.
40. Gard B, Bout A, Pierre P. Release strategies of *Trissolcus basal* (Scelionidae) in protected crops against *Nezara viridula* (Pentatomidae): less is more. *Crop Prot*. 2022;161:106069. <https://doi.org/10.1016/j.cropro.2022.106069>.
41. Ederli L, Brunetti C, Centritto M, Colazza S, Frati F, Loreto F, et al. Infestation of broad bean (*Vicia faba*) by the green stink bug (*Nezara viridula*) decreases shoot abscisic acid contents under well-watered and drought conditions. *Front Plant Sci*. 2017;8:1–12. <https://doi.org/10.3389/fpls.2017.00959>.
42. Kaspi R, Mossinson S, Drezner T, Kamensky B, Yuval B. Effects of larval diet on development rates and reproductive maturation of male and female mediterranean fruit flies. *Physiol Entomol*. 2002;27:29–38. <https://doi.org/10.1046/j.1365-3032.2001.00264.x>.
43. Xie J, De Clercq P, Pan C, Li H, Zhang Y, Pang H. Larval nutrition-induced plasticity affects reproduction and gene expression of the Ladybeetle, *Cryptolaemus montrouzieri*. *BMC Evol Biol*. 2015;15:276. <https://doi.org/10.1186/s12862-015-0549-0>.
44. Alinç T, Peri E, Torta L, Guarino S, Colazza S, Lievens B, et al. Root inoculation with beneficial soil microbes enhances indirect plant defences induced by insect feeding and egg deposition. *Funct Ecol*. 2024;38:1811–21. <https://doi.org/10.1111/1365-2435.14594>.
45. Van Hee S, Alinç T, Weldegergis BT, Dicke M, Colazza S, Peri E, et al. Differential effects of plant-beneficial fungi on the attraction of the egg parasitoid *Trissolcus basal* in response to *Nezara viridula* egg deposition. *PLoS ONE*. 2024;19:e0304220. <https://doi.org/10.1371/journal.pone.0304220>.
46. Harun-Or-Rashid M, Chung YR. Induction of systemic resistance against insect herbivores in plants by beneficial soil microbes. *Front Plant Sci*. 2017;8:1–11. <https://doi.org/10.3389/fpls.2017.01816>.

47. Hermosa R, Belén Rubio M, Cardoza RE, Nicolás C, Monte E, Gutiérrez S. The contribution of *Trichoderma* to balancing the costs of plant growth and defense. *Int Microbiol*. 2013;16:69–80. <https://doi.org/10.2436/20.1501.01.18.1>.
48. Zhou D, Huang X, Guo J, Dos-Santos ML, Vivanco JM. *Trichoderma gamsii* affected herbivore feeding behaviour on *Arabidopsis thaliana* by modifying the leaf metabolome and phytohormones. *Micro Biotechnol*. 2018;11:1195–206. <https://doi.org/10.1111/1751-7915.13310>.
49. Mashabela MD, Tugizimana F, Steenkamp PA, Piater LA, Dubery IA, Terefe T, et al. Metabolomic evaluation of PGPR defence priming in wheat (*Triticum aestivum* L.) cultivars infected with *Puccinia striiformis* F. Sp. *tritici* (stripe rust). *Front Plant Sci*. 2023;14:1–11. <https://doi.org/10.3389/fpls.2023.1103413>.
50. Conrath U, Beckers GJM, Flors V, García-Agustín P, Jakab G, Mauch F, et al. Priming: getting ready for battle. *Mol Plant Microbe Interact*. 2006;19:1062–71. <https://doi.org/10.1094/MPMI-19-1062>.
51. Mauch-Mani B, Baccelli I, Luna E, Flors V. Defense priming: an adaptive part of induced resistance. *Annu Rev Plant Biol*. 2017;68:485–512. <https://doi.org/10.1146/annurev-arplant-042916-041132>.
52. Karban R. The ecology and evolution of induced resistance against herbivores. *Funct Ecol*. 2011;25:339–47. <https://doi.org/10.1111/j.1365-2435.2010.01789.x>.
53. Kloth KJ, Dicke M. Rapid systemic responses to herbivory. *Curr Opin Plant Biol*. 2022;68:102242. <https://doi.org/10.1016/j.cpb.2022.102242>.
54. Mostafa S, Wang Y, Zeng W, Jin B. Plant responses to herbivory, wounding, and infection. *Int J Mol Sci*. 2022;23:7031. <https://doi.org/10.3390/ijms23137031>.
55. Douma JC, Vermeulen PJ, Poelman EH, Dicke M, Anten NPR. When does it pay off to prime for defense? A modeling analysis. *New Phytol*. 2017;216:782–97. <https://doi.org/10.1111/nph.14771>.
56. Vogt T. Phenylpropanoid biosynthesis. *Mol Plant*. 2010;3:2–20. <https://doi.org/10.1093/mp/ssp106>.
57. Sharma A, Shahzad B, Rehman A, Bhardwaj R, Landi M, Zheng B. Response of phenylpropanoid pathway and the role of polyphenols in plants under abiotic stress. *Molecules*. 2019;24:1–22. <https://doi.org/10.3390/molecules24132452>.
58. Dixon RA, Achnine L, Kota P, Liu C, Reddy MSS, Wang L. The phenylpropanoid pathway and plant defence—a genomics perspective. *Mol Plant Pathol*. 2002;3:371–90. <https://doi.org/10.1046/j.1364-3703.2002.00131.x>.
59. Dudareva N, Klempien A, Muhlemann JK, Kaplan I. Biosynthesis, function and metabolic engineering of plant volatile organic compounds. *New Phytol*. 2013;198:16–32. <https://doi.org/10.1111/nph.12145>.
60. Ramaroson M, Koutouan C, Helesbeux J, Le Clerc V, Hamama L, Geoffriau E, et al. Role of phenylpropanoids and flavonoids in plant resistance to pests and diseases. *Molecules*. 2022;27:8371. <https://doi.org/10.3390/molecules27238371>.
61. Al-Khayri JM, Rashmi R, Toppo V, Chole PB, Banadka A, Sudheer WN, et al. Plant secondary metabolites: the weapons for biotic stress management. *Metabolites*. 2023;13:1–37. <https://doi.org/10.3390/metabo13060716>.
62. Xia T, Liu Y, Lu Z, Yu H. Natural coumarin shows toxicity to *Spodoptera litura* by inhibiting detoxification enzymes and glycometabolism. *Int J Mol Sci*. 2023;24. <https://doi.org/10.3390/ijms241713177>.
63. Araújo MO, Pérez-Castillo Y, Oliveira LHG, Nunes FC, de Sousa DP. Larvicidal activity of cinnamic acid derivatives: investigating alternative products for *Aedes aegypti* L. control. *Molecules*. 2021;26:1–21. <https://doi.org/10.3390/MOLECULES26010061>.
64. Gerlin L, Baroukh C, Genin S. Polyamines: double agents in disease and plant immunity. *Trends Plant Sci*. 2021;26:1061–71. <https://doi.org/10.1016/j.tplants.2021.05.007>.
65. Chen D, Shao Q, Yin L, Younis A, Zheng B. Polyamine function in plants: metabolism, regulation on development, and roles in abiotic stress responses. *Front Plant Sci*. 2019;9:1–13. <https://doi.org/10.3389/fpls.2018.01945>.
66. García PA, De Oliveira AB, Batista R. Occurrence, biological activities and synthesis of Kaurane diterpenes and their glycosides. *Molecules*. 2007;12:455–83. <https://doi.org/10.3390/12030455>.
67. Li R, Morris-Natschke SL, Lee KH. Clerodane diterpenes: sources, structures, and biological activities. *Nat Prod Rep*. 2016;33:1166–226. <https://doi.org/10.1039/c5np00137d>.
68. Chen XL, Sun MC, Chong SL, Si JP, Wu LS. Transcriptomic and metabolomic approaches deepen our knowledge of plant–endophyte interactions. *Front Plant Sci*. 2022;12:1–25. <https://doi.org/10.3389/fpls.2021.700200>.
69. Richards LA, Glassmire AE, Ochsenrider KM, Smilanich AM, Dodson CD, Jeffrey CS, et al. Phytochemical diversity and synergistic effects on herbivores. *Phytochem Rev*. 2016;15:1153–66. <https://doi.org/10.1007/s11101-016-9479-8>.
70. McLean AHC, Parker BJ, Hrčák J, Henry LM, Godfray HCJ. Insect symbionts in food webs. *Philosophical Trans Royal Soc B: Biol Sci*. 2016;371. <https://doi.org/10.1098/rstb.2015.0325>.
71. Rosenberg E, Zilber-Rosenberg I. Microbes drive evolution of animals and plants: the hologenome concept. *mBio*. 2016;7. <https://doi.org/10.1128/mBio.01395-15>.
72. Tada A, Kikuchi Y, Hosokawa T, Musolin DL, Fujisaki K, Fukatsu T. Obligate association with gut bacterial symbiont in Japanese populations of the Southern green Stinkbug *Nezara viridula* (Heteroptera: Pentatomidae). *Appl Entomol Zool*. 2011;46:483–8. <https://doi.org/10.1007/s13355-011-0066-6>.
73. Geerincx MWJ, Van Hee S, Gloder G, Crauwels S, Colazza S, Jacquemyn H, et al. Diversity and composition of the Microbiome associated with eggs of the Southern green Stinkbug, *Nezara viridula* (Hemiptera: Pentatomidae). *Microbiologyopen*. 2022;11:e1337. <https://doi.org/10.1002/mbo3.1337>.
74. Meesters C, Cialdella L, Ingels R, Jacquemyn H, Lievens B. Cultivar-dependent effects of plant-beneficial fungi on plant nutrient composition and feeding damage by *Nesidiocoris tenuis*. *Plant Soil*. 2023;492:177–90. <https://doi.org/10.1007/s11104-023-06165-6>.
75. Wilberts L, Vuts J, Caulfield JC, Thomas G, Birkett MA, Herrera-Malaver B et al. Impact of endophytic colonization by entomopathogenic fungi on the behavior and life history of the tobacco peach aphid *Myzus persicae* var. *nicotianae*. Agarwala N, editor. *PLoS One*. 2022;17: e0273791. <https://doi.org/10.1371/journal.pone.0273791>.
76. Doneanu CE, Chen W, Mazzeo JR, Ds OR. UPLC/MS monitoring of water-soluble vitamin Bs in cell culture media in minutes. *Water Application Note*. 2011; 1–7.
77. Chambers MC, MacLean B, Burke R, Amodei D, Ruderman DL, Neumann S, et al. A cross-platform toolkit for mass spectrometry and proteomics. *Nat Biotechnol*. 2012;30:918–20. <https://doi.org/10.1038/nbt.2377>.
78. Heuckeroth S, Damiani T, Smirnov A, Mokshyna O, Brungs C, Korf A, et al. Reproducible mass spectrometry data processing and compound annotation in MZmine 3. *Nat Protoc*. 2024. <https://doi.org/10.1038/s41596-024-00996-y>.
79. Myers OD, Sumner SJ, Li S, Barnes S, Du X. One step forward for reducing false positive and false negative compound identifications from mass spectrometry metabolomics data: new algorithms for constructing extracted ion chromatograms and detecting chromatographic peaks. *Anal Chem*. 2017;89:8696–703. <https://doi.org/10.1021/acs.analchem.7b00947>.
80. Pakkiri Shah AK, Walter A, Ottosson F, Russo F, Navarro-Diaz M, Boldt J, et al. Statistical analysis of feature-based molecular networking results from non-targeted metabolomics data. *Nat Protoc*. 2024. <https://doi.org/10.1038/s41596-024-01046-3>.
81. R Core Team. R: A language and environment for statistical computing. R foundation for statistical computing. 2019. Available: <https://www.r-project.org/>.
82. Tyanova S, Temu T, Cox J. The MaxQuant computational platform for mass spectrometry-based shotgun proteomics. *Nat Protoc*. 2016;11:2301–19. <https://doi.org/10.1038/nprot.2016.136>.
83. Tyanova S, Temu T, Sinitcyn P, Carlson A, Hein MY, Geiger T, et al. The perseus computational platform for comprehensive analysis of (pro)teomics data. *Nature methods*. Nature Publishing Group; 2016. pp. 731–40. <https://doi.org/10.1038/nmeth.3901>.
84. Tugizimana F, Steenkamp PA, Piater LA, Dubery IA. A conversation on data mining strategies in LC-MS untargeted metabolomics: Pre-processing and pre-treatment steps. *Metabolites*. 2016;6. <https://doi.org/10.3390/metabo6040040>.
85. Oksanen J, Blanchet FG, Friendly M, Kindt R, Legendre P, McGlinn D et al. *vegan: Community Ecology Package*. 2020. https://doi.org/10.1007/978-94-024-1179-9_301576.

Publisher's note

Springer Nature remains neutral with regard to jurisdictional claims in published maps and institutional affiliations.